

***In Vitro* anticandidal efficiency of newly synthesized zinc oxide/chitosan/vancomycin nanocomposite using *Bacillus Licheniformis* compared to fluconazole**Mohamed I Abou-Dobara¹, Zakaria AM Baka¹, Shimaa M El-Salamony¹, and Mohamed M El-Zahed^{1,*}¹Department of Botany and Microbiology, Faculty of Science, Damietta University, New Damietta, Egypt^{*}Corresponding author: mohamed.marzouq91@du.edu.eg

Received 16 July 2025

Revised 29 September 2025

Accepted 18 November 2025

Abstract

The zinc oxide/chitosan nanocomposite functionalized with vancomycin (ZnO/CS/VA), which acts as a novel anticandidal modifier, was prepared using an environmentally friendly technique. Zinc oxide nanoparticles (ZnO NPs) were biosynthesized using *Bacillus licheniformis* ATCC 4527 and then linked to chitosan (CS) and vancomycin (VA) through a green chemical method. Several methods were utilized to characterize the prepared nanocomposite. UV-Vis spectroscopy results indicated an absorption peak at 348 nm. Fourier transform infrared spectroscopy (FTIR) and X-ray diffractometer (XRD) analyses demonstrated that the material matrix of the nanocomposite included ZnO NPs and various active groups. Transmission electron microscopy (TEM) images showed that the ZnO/CS/VA nanocomposite was spherical-shaped with a size range of 56-80 nm. The anticandidal effect of ZnO/CS/VA, used as a modifier to enhance antimicrobial activity, was tested against *Candida albicans* ATCC 10231. ZnO/CS/VA exhibited significant anticandidal activity in the agar well-diffusion test, minimum inhibitory concentration (MIC), and minimum fungicidal concentration (MFC) compared to the standard drug fluconazole. As the ZnO/CS/VA dose and the anticandidal inhibition increased, the antimicrobial activity became reliant on the nanocomposite dose. Five μ g/mL was enough to cause complete biocidal action against *Candida albicans*, while 25 μ g/mL of fluconazole was required. TEM micrographs of ZnO/CS/VA-treated *Candida albicans* showed various malformations and distortions in cell structure, including damage to the cell wall and the presence of vacuoles, indicating its potent antimicrobial effects. The results suggest that the combination of zinc oxide/chitosan nanocomposite and vancomycin could serve as an effective biomaterial for antifungal treatment and other medical applications.

Keywords: Anticandidal activity, *Bacillus licheniformis*, Nanocomposite, Vancomycin, ZnO NPs**1. Introduction**

The term antimicrobial resistance (AMR) describes a pathogen's ability to become resistant to medications intended to eradicate it, making the illnesses they cause more challenging to cure and increasing the risk of disease spread and death. AMR is therefore considered one of the biggest and most pervasive threats to society, the environment, and human health [1]. The misuse and abuse of antibiotics in healthcare, veterinary medicine, and agriculture have led to the development of AMR [2]. AMR is a complex phenomenon that results from the interaction of genetic factors and selective pressures in microbial populations. Stronger strains are created as a result of this process, making it easier for antibiotic-resistant microbes to spread unchecked through various channels. It is estimated that a staggering 4.95 million people worldwide will die from drug-resistant diseases in 2019, with low- and middle-income countries (LMICs), particularly those in Sub-Saharan Africa, bearing the brunt of the clinical burden [3]. If no action is taken, it is projected that AMR will cause 10 million deaths annually by 2050 [4].

Candida albicans is one of the few microorganisms that can cause disease in humans and animals. The majority of people have this asymptomatic member of the healthy microbiota colonizing their skin, oral cavity,

reproductive tract, and gastrointestinal tract [5]. Because it coexists in harmony with other local microbiota members, *C. albicans* is frequently benign in people with robust immune systems. However, *C. albicans* can multiply and cause illness if there are changes in the host microbiota (such as the presence of antibiotics), the host immune response (such as microbial infection or immunosuppressive medication), or the local environment (such as pH or nutritional changes). Thrush, vaginal yeast infections, and diaper rash are examples of superficial mucosal and dermal *Candida* infections. Hematogenously disseminated infections with high death rates (up to 40% in certain situations) have been documented. *Candida* infections are particularly dangerous for healthy individuals with implanted medical devices and immunocompromised individuals. Various studies have recorded the microbial resistance of *C. albicans* to several current anticandidal agents, such as fluconazole and voriconazole [6].

Many researchers have garnered attention for utilizing nanotechnology to address the issue of AMR [7–9]. The rapidly expanding field of nanotechnology aims to develop new chemicals and molecules at the nanoscale level, with applications across various scientific and research fields. A “nano” is equivalent to one billionth of a meter in terms of measurement. Nanoparticles (NPs) refers to solid particles or collections of atoms, that range in size from one to one hundred nanometers. The term “nano” comes from the Greek word “dwarf,” indicating something extremely small. Due to their unique properties, NPs have a wide range of applications. NPs differ not only in material but also in size, shape, and dimension. The chemical characteristics of these substances determined their potential uses, including reactivity with the target, stability and susceptibility to environmental factors such as heat, light, moisture, and the surrounding environment. The antibacterial, antifungal, disinfecting, and antiviral properties of NPs makes them suitable for use in biological and environmental settings. The range of applications for which NPs can be utilized is influenced by their ability to oxidize, reduce, ignite, and exhibit anti-corrosive qualities [10–12].

There are two methods for creating nanomaterials. The first method is the top-down approach, which involves mechanical milling, laser ablation, and thermal breakdown, to break down a material into its constituent atoms. This technique allows for large amounts of material to be divided into minuscule, nanoscale fragments. Secondly, the bottom-up method of nanofabrication, involves the use of physical or chemical forces at the nanoscale, as well as self-assembly techniques to combine building components and create useful structures [13]. Pyrolysis, sol-gel, and biosynthesis are examples of bottom-up methods that begin at the atomic level and progress to the NPs level. However, nonbiological methods may involve high costs, high energy consumption, complex protocols, and additional follow-up steps such as purification and stabilization processes. Additionally, they could require the use of toxic solvents and reactants. Biological methods are an environmentally friendly alternative to chemical and physical synthesis, often referred to as “green synthesis.” These methods utilize microorganisms, plants or their extracts to biosynthesize NPs [11]. This method is biocompatible, and rapid, contains biomolecules that act as both reducing and capping agents, and avoids toxic chemicals. Inorganic NPs can be produced by microbes either extracellularly or intracellularly, often at stunningly shaped nanoscale sizes. The main mechanisms of microbial resistance to toxic heavy metals involve chemical detoxification and energy-dependent ion efflux from the cell. This is achieved through the action of membrane proteins functioning as ATPase, chemiosmotic cations, or proton anti-transporters [13].

Probiotics are live microorganisms that can improve the health of the host when consumed in sufficient quantities. Some common probiotics include *Lactobacillus* species (such as *L. acidophilus*, *L. casei*, and *L. rhamnosus*) and *Bifidobacterium* species (like *B. bifidum* and *B. longum*). These probiotics have the ability to produce NPs of various metals like Ag, Cu, Au, Zn, Se, and TiO₂, which have been shown to have several positive health effects. These effects include high stability of NPs, prevention of allergic reactions, enhancement intestinal immune function, antioxidative and antitumorigenic effects, and a hypocholesterolemic characteristic. Numerous studies have demonstrated these benefits [14–16]. Among the members of the *Bacillus* genus, *B. licheniformis* is a unique species that produces a wide range of antibiotic compounds. Dysbacteriosis caused by various illnesses, can be treated using this bacterium as a probiotic. The ability of *B. licheniformis* to produce a variety of compounds with antibacterial, antioxidant, and immunomodulatory qualities is associated with its benefits as a probiotic [17]. Abinaya *et al.* [18] utilized the exopolysaccharides (EPS) from the probiotic strain *B. licheniformis* Dabhb1 to synthesize ZnO NPs in a novel and efficient manner. According to Gomaa [19], microorganisms have the ability to produce and release proteins and enzymes that can stabilize the NPs and decrease the concentration of metal ions during the microbial synthesis of ZnO NPs.

Metal oxide NPs, such as zinc oxide nanoparticles (ZnO NPs), offer new potential biological applications ranging from treatment to detection. The mechanical, regenerative, and antibacterial properties of these NPs are just a few examples of their versatile uses. The applications include coating dental implants, improving the stability of local drug delivery agents, and enhancing the antimicrobial properties of various materials [15,20–23]. ZnO NPs have a molecular weight of 81.38 g/mol and are white, odorless particles. The drug is generally recognized as safe (GRAS), according to the Food and Drug Administration (FDA). The antimicrobial action of ZnO NPs and other NPs against *C. albicans* has been reported in previous studies [14, 24]. However, microbes may become resistant to antimicrobial NPs in a manner similar to how they are known to become resistant to

antibiotics. Nevertheless, NPs have been found to be potent antimicrobial agents. Several investigations have revealed that bacteria have begun to show resistance to NPs including silver NPs and ZnO NPs [25]. In the current study, a novel nanocomposite was created by combining ZnO NPs with vancomycin (VA) in the presence of chitosan (CS). The study aimed to examine its anticandidal properties in comparison to the standard anticandidal fluconazole. While VA is a potent antibiotic that primarily targets Gram-positive bacteria by inhibiting cell wall synthesis, some studies suggest that antibiotics may have a synergistic effect against certain fungi, including *Candida* sp. [24]. The mechanism does not involve direct fungicidal action as seen with bacteria, but rather a potential for membrane-disrupting or anti-biofilm activity. This weakening of the fungus can make it more susceptible to other treatments.

2. Materials and methods

2.1 Intracellular biosynthesis of zinc oxide nanoparticles

Sterile nutrient broth flasks were inoculated with 0.5 McFarland ($1-2 \times 10^8$ CFU/mL) from *B. licheniformis* ATCC 4527. The flasks were then incubated for 24 hrs. at 37°C and 150 rpm. After the incubation period, cell pellets were collected by centrifuging of the bacterial cultures for 15 min at 5000 rpm followed by washing them at least three times with distilled water. The cell pellets were resuspended in a $\text{Zn}(\text{NO}_3)_2$ solution (3 mM, $\geq 99.0\%$, Sigma-Aldrich, USA) and incubated at 37°C and 150 rpm for 24 hrs. under dark conditions. After incubation, the reaction mixture was centrifuged at 4000 rpm for 15 min to remove the supernatant. The bacterial pellets were washed at least three times with distilled water and then ultrasonicated to extract ZnO NPs. The tubes were centrifuged at 4000 rpm for 5 min, and the supernatant containing ZnO NPs, was transferred to new tubes. The ZnO NPs solution was then dried at 80°C for 24 hrs. and subsequently calcined at 500°C for 3 hrs. [19].

2.2 Synthesis of zinc oxide/chitosan nanocomposite

At room temperature, 6 mg of CS (MW 50–190 KDa, Sigma-Aldrich, USA) was dissolved in 10 mL of 1% acetic acid and stirred for 15 min until completely dissolved. Simultaneously, 6 mg of ZnO NPs was ultrasonicated in 10 mL of distilled water for 15 min using an Elmasonic S100H ultrasonic bath (50/60 Hz, Germany). Afterwards, the previously prepared solutions were mixed in a 1:1 v/v ratio, stirred for 20 min, and then ultrasonicated for additional 15 min [8].

2.3 Functionalizing of zinc oxide/chitosan nanocomposite with vancomycin

At room temperature, 6 mg of antibiotic VA (Mylan Pharmaceuticals Ltd., Ireland) was added to a zinc oxide/chitosan nanocomposite solution and stirred at 500 rpm for 20 min. After 6 hrs., the drug loaded nanocomposite was centrifuged at 5000 rpm, and the residue was washed three times with distilled water. Finally, the product was dried at 50°C for 24 hrs. [24].

2.4 Characterization of zinc oxide/chitosan/vancomycin nanocomposite

The zinc oxide/chitosan/vancomycin nanocomposite (ZnO/CS/VA) was examined and studied using a double beam spectrum UV–Vis spectrophotometer V-630 (JASCO, UK). Fourier transform infrared spectroscopy (FTIR, FT/IR-4100type A) was conducted at the Central Lab of the Chemistry Department of Damietta University in Egypt. The characteristics of ZnO/CS/VA were investigated using an X-ray diffractometer (model LabX XRD-6000, Shimadzu, Japan) at the Central Metallurgical Research and Development Institute (CMRDI) in Cairo, Egypt. Transmission electron microscopy (TEM) was conducted using a device (200 kV, TEM JEOL JEM-2100, Japan), and zeta potential analysis was performed using a zeta potential analyzer (Malvern Zetasizer Nano-ZS90, Malvern, UK) at the Center for Excellence in Research of Advanced Agricultural Sciences (CERAAS) at Damietta University in Egypt.

2.5 Anticandidal activity using agar well diffusion method

The *C. albicans* ATCC 10231 strain was provided by the Microbiology Lab at the Faculty of Science, Damietta University. It was used as a model to test the anticandidal properties of ZnO NPs and ZnO/CS/VA according to CLSI standards [26]. Nutrient agar (Oxoid, UK) plates were prepared and inoculated with the tested yeast (1×10^6 CFU/mL). Solutions of 150 $\mu\text{g}/\text{mL}$ of ZnO NPs, CS, and ZnO/CS/VA were prepared in sterile distilled water and applied (100 μl) to wells (5 mm) in the nutrient agar plates. Fluconazole (Pfizer Inc., USA) was used as a standard anticandidal agent. The agar plates were then incubated at 28°C for 48 hrs. After the incubation period, zones of inhibition (ZOI) were measured and recorded. The experiment was conducted in triplicates.

2.6 Minimum inhibition concentration

The minimum inhibitory concentration (MIC) for ZnO NPs and ZnO/CS/VA was determined using the broth dilution method [27]. A total of 50 mL of nutrient broth medium (Oxoid, UK) supplemented with varying doses (0–50 µg/mL) of ZnO NPs, CS, fluconazole, or ZnO/CS/VA was inoculated with 100 µl of overnight *C. albicans* culture and incubated for 24 hrs. The culture was then further incubated for additional 24 hrs. at 28°C and 150 rpm. MIC values (no apparent growth) were determined at 600 nm using UV-Vis spectrophotometry.

2.7 Minimum fungicidal concentration

The minimum fungicidal concentration (MFC) for ZnO NPs and ZnO/CS/VA was also investigated [14]. Nutrient agar plates were prepared and inoculated with 10 µl of each MIC set using the pour plate method, then incubated for 48 hrs. at 28°C. After the incubation period, the plates were observed and MFC values were recorded.

2.8 Ultrastructural studies of ZnO/CS/VA-treated *C. albicans*

For 2 hrs. at 28°C in nutrient broth medium, the *C. albicans* cultures were subjected to ZnO/CS/VA (MFC value). After being cleaned and treated with 2.5% glutaraldehyde and 0.1 M cacodylate buffer (pH 7), the cells were transferred to the Central Laboratory, Electron Microscope Unit, Mansoura University, Egypt, for ultrastructure analysis and observation. After the fixative was removed, 0.1 M buffer was added for washing, and 2% osmium tetroxide was used to fix the sample for 90 min. The fixed cells were dehydrated using a graded series of ethanol. Following drying, the cells were submerged for one hour in a 1:1 Epon-Araldite mixture, and the mixture was then polymerized for twenty-four hrs. at 65°C. A TEM was used to view the cells on carbon-coated copper grids (Type G 200, 3.05 µm diameter, TAAP, U.S.A.) after they had been sectioned using an ultramicrotome (50 µm) and double-stained with lead citrate (0.2%) and uranyl acetate (2%) for 5 min.

2.9 Statistical analysis

The data was statistically analyzed using SPSS software, specifically version 18. The mean ± standard deviation (SD) was used to present the results of each experiment following Duncan's multiple range test and one-way analysis of variance (ANOVA). A significance level of $p < 0.05$ was utilized.

3. Results and discussion

3.1 Synthesis and characterization of ZnO/CS/VA

The goal of biosystems is to utilize microorganisms in various biotechnology applications, including the creation of nanomaterials. Various microorganisms, such as bacteria, fungi, and algae, act as biocatalysts in a biosystem to convert bulk matter into materials on the nanoscale. Bacteria are used as excellent nano-factories due to their rapid growth, small size, and easy cultural conditions. They also have the ability to control the shape and size of the produced NPs. *B. licheniformis* ATCC 4527 biosynthesized ZnO NPs intracellularly within 24 hrs. The color change and white colloidal precipitate formation confirmed the formation of ZnO NPs (Figure 1). The solution was white and clear in distilled water, and the color of the reaction changed to whitish and cloudy after Zn^{2+} was added, indicating that Zn^{2+} was reduced to ZnO NPs. Analysis of ZnO/CS/VA using UV-Vis spectroscopy showed a distinct peak at 348 nm. Markus *et al.* [28] proposed that biological substances released into the supernatant by the bacteria and functional groups on the bacterial cell were responsible for the reduction of Zn^{2+} to ZnO NPs. Ali *et al.* [29] developed a simple and inexpensive approach for the synthesis of ZnO NPs over 24 hrs., displaying absorption peaks in the range of 350–380 nm. Meanwhile, Salman *et al.* [30] reported the biosynthesis of ZnO NPs at 80°C using *Lactobacillus* sp. over 24 hrs.

The FT-IR spectrum of ZnO/CS/VA confirmed the presence of amines as a capping agent, as shown in Figure 2. Primary amines and asymmetric amines revealed stretching peaks at 1553–1665 cm^{-1} and 2941 cm^{-1} , respectively. The presence of carbonyl groups from amino acid residues in proteins has a strong ability to bind metal from metal NPs, such as capping ZnO NPs residues, which prevents the accumulation and aggregation of NPs. Hydroxyl groups appear at 3258 cm^{-1} while esters and carboxylic acids appear at 1075–1335 cm^{-1} . The ZnO vibration stretching band was observed at several peaks ranging from 460–800 cm^{-1} confirming the successful loading of ZnO with ZnO/CS nanocomposite. This aligns with the FT-IR results and explanations provided by Abd El-Nour *et al.* [16, 21] and Fozouni *et al.* [31].

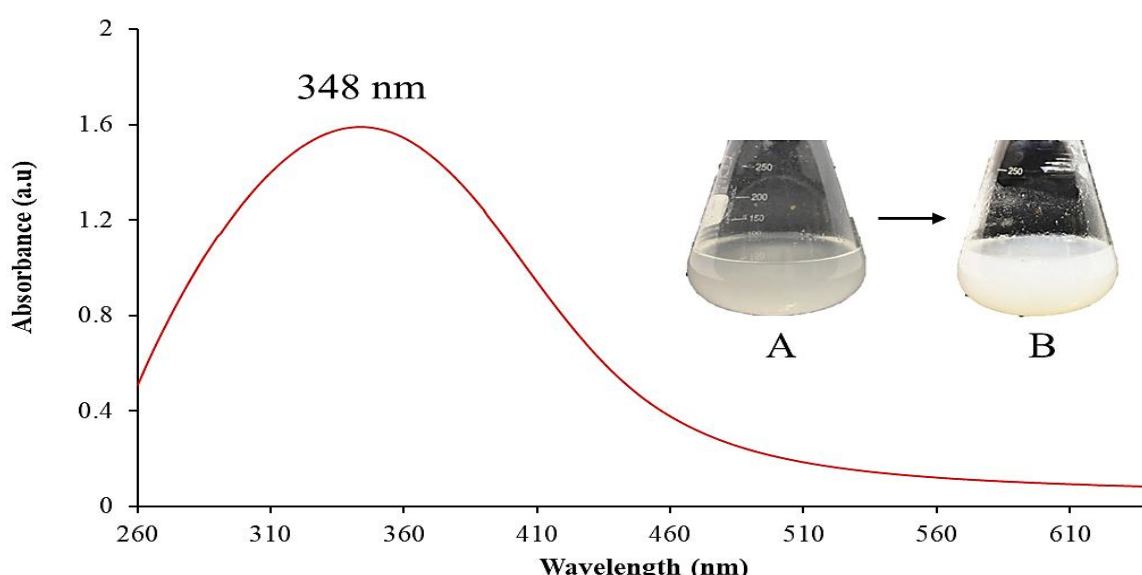


Figure 1 The UV-Vis spectrum of ZnO/CS/VA, showing an absorption peak at 348 nm. (A) The color of the reaction mixture at the beginning of the biosynthesis process. (B) The color change into white colloidal precipitate after the production of ZnO NPs.

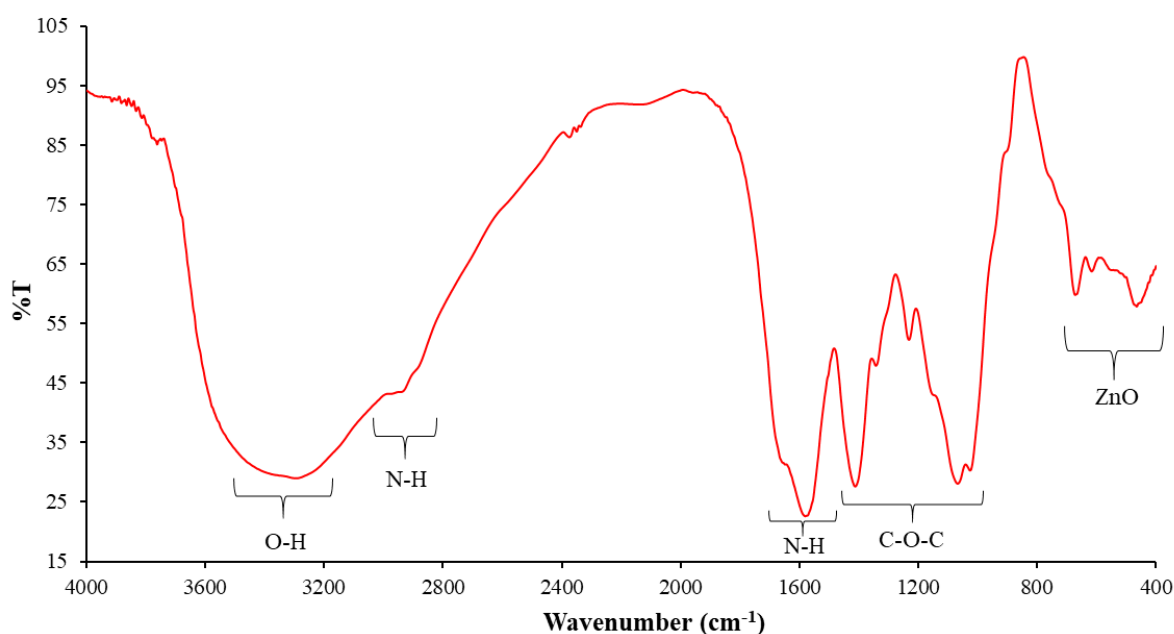


Figure 2 FTIR spectrum of ZnO/CS/VA, showing peaks of hydroxyl, amines, esters, carboxylic acids, and ZnO NPs at 3258 cm^{-1} , $1553\text{-}1665\text{ cm}^{-1}$, 2941 cm^{-1} , $1075\text{-}1335\text{ cm}^{-1}$, and $460\text{-}800\text{ cm}^{-1}$, respectively.

An XRD spectrum of ZnO/CS/VA displayed the purity and well-crystalline nature of the prepared nanocomposite (Figure 3). Sharp peaks at 31.91° , 34.62° , 56.67° , 66.39° , and 75.44° correspond to the lattice planes (100), (102), (110), (200), and (202), respectively, confirming the integration of ZnO NPs in ZnO/CS/VA. The peaks of ZnO NPs matched the Joint Committee of Powder Diffraction Standards (JCPDS) card No. 36-1451. The Debye-Scherrer equation ($D=k\lambda/\beta\cos\theta$) was used to calculate the average particle size, where D represents particle size, K is a constant (0.94), λ is the x-ray wavelength, β is full width at half maximum, and θ is the angle of diffraction. The calculation indicated an average particle size of 79.38 nm. No additional impurity-related diffraction peaks were detected, confirming the high purity of the produced materials.

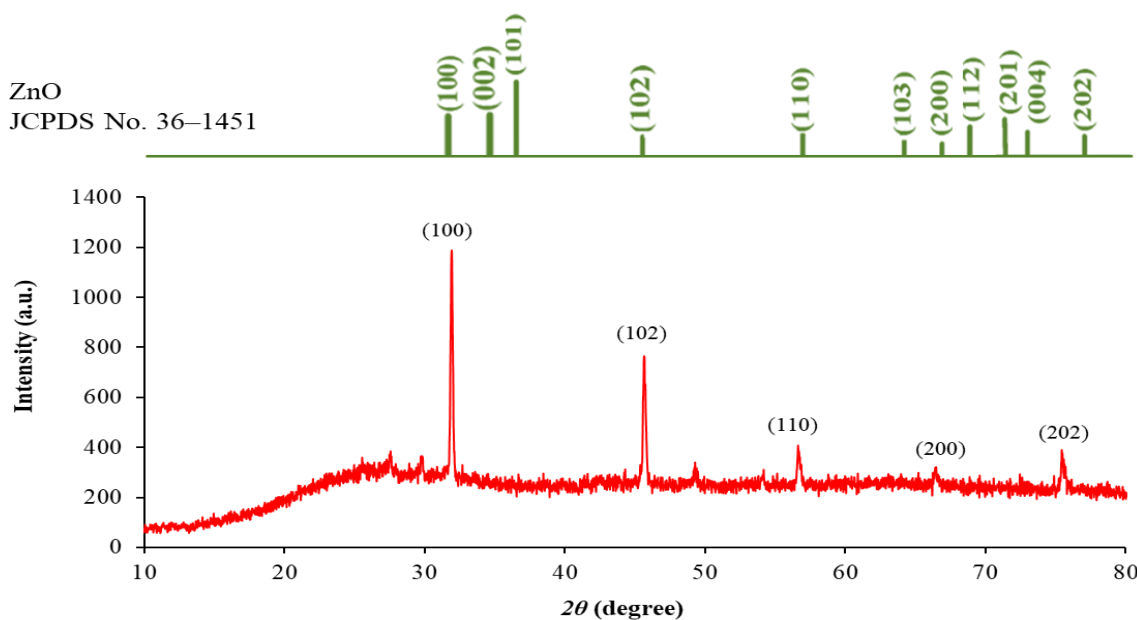


Figure 3 XRD patterns of ZnO/CS/VA (Peaks are well marked at 100, 102, 110, 200, and 202, showing different crystalline planes).

The TEM is an essential instrument for evaluating the size and shape of the produced NPs. Figure 4 displays a TEM micrograph of ZnO/CS/VA. The particles are spherical-shaped NPs with an average diameter of 78 ± 2.3 nm, which aligns with the results of the Debye-Scherrer equation. Smaller NPs have a stronger antimicrobial effect than larger ones. They can harm microbial protoplasts by condensing DNA molecules, preventing replication, and deactivating enzymes and metabolism [32]. These findings demonstrate that the process used in this work to produce pure ZnO NPs is efficient. Furthermore, the results show that the diffraction peaks became smaller and more intense as the annealing temperature increased, suggesting that the ZnO NPs produced had an excellent crystalline structure. In comparison to the current study, the average size of ZnO/CS was found to be 338.7 nm, as reported by Mehta *et al.* [33].

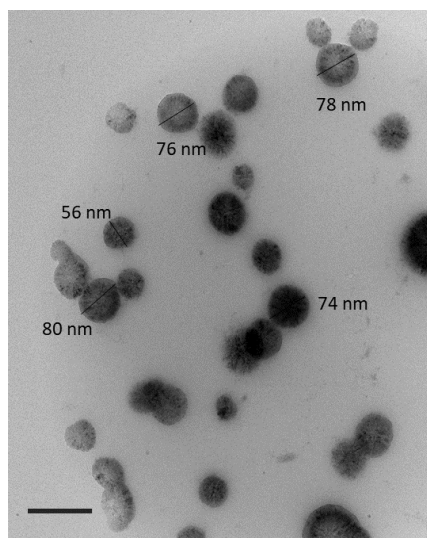


Figure 4 TEM of ZnO/CS/VA with scale bar = 100 nm. ZnO NPs appeared as spherical-shaped NPs with an average diameter of 78 ± 2.3 nm.

The stability of the NPs was demonstrated by the magnitude of the zeta potential value. The zeta potential results showed the negative charge of the green synthesized nanocomposite (-17.8 mV), as shown in Figure 5. The significant negative charge of zeta potential prevents the agglomeration of NPs, which is the cause of their increased stability. Studies on NPs synthesis clearly indicate that the stability of particles is moderately stable.

Iqtedar *et al.* [34] documented that the zeta potential of NPs is considered almost neutral when it falls between -10 mV and $+10$ mV.

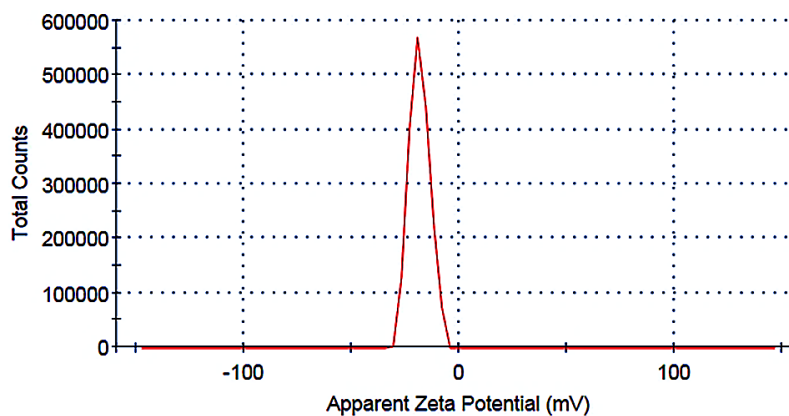


Figure 5 Zeta potential of ZnO/CS/VA, showing negative charge -17.8 mV.

3.2 Anticandidal activity of ZnO/CS/VA compared to fluconazole

According to the agar well diffusion test, ZnO/CS/VA exhibited superior anticandidal activity against the tested *C. albicans* with an inhibition zone of 31 ± 0 mm compared to the standard drug fluconazole, which resulted in an inhibition zone of 18 ± 0.03 mm (Figure 6 and Table 1). It was also observed that *C. albicans* exhibited complete resistance to CS (no inhibition zone) and only a weak anticandidal effect from ZnO NPs (9 ± 0.14 mm). These findings are consistent with a study by Kyu Aung & Thida-Htun [35], which synthesized a ZnO/CS nanocomposite using the co-precipitation method and reported an inhibition zone of 30 mm against *C. albicans*, while CS showed no inhibition zone against the same strain. Ali *et al.* [29] reported the anticandidal action of chemically formulated ZnO/CS and physically prepared ZnO/CS nanocomposite with inhibition zones ranging from 12-15 mm and 15-21 mm. Ghosh *et al.* [6] recorded the complete resistance of *C. albicans* to fluconazole and voriconazole. However, during the current study, fluconazole showed a moderate anticandidal potential against *C. albicans*. It has been reported to have harmful side effects on human health, such as hepatotoxicity and hormone-related effects. These effects include alopecia, oligospermia, azoospermia, hypokalemia, and hyponatremia. The novelty does not lie in any single component, but in the specific combination and synergistic effect of the three materials: ZnO NPs, CS, and VA. ZnO NPs are known for their broad antimicrobial and antifungal properties. CS is a biocompatible polymer with its own antifungal and film-forming capabilities [8]. VA provides potent antibacterial and potential anti-biofilm activity. The novelty lies in the development of a single, multifunctional nanocomposite that combines the strengths of each component. This composite is designed to have a more potent and broad-spectrum antimicrobial action than any of its individual components, representing a significant advancement over existing, single-component materials. Although VA is a potent antibiotic that primarily targets Gram-positive bacteria by inhibiting the formation of their cell walls, recent research suggests that it may also work in conjunction with other antimicrobial agents to combat pathogenic fungi. Unlike bacteria which have a direct fungicidal effect, VA may act through anti-biofilm or membrane-disrupting properties that weaken the fungus and enhance its susceptibility to other treatments.



Figure 6 Anticandidal activity of fluconazole, ZnO NPs, CS, and ZnO/CS/VA against *C. albicans*.

Table 1 Agar well diffusion method of fluconazole, ZnO NPs, CS, and ZnO/CS/VA against *C. albicans*.

Antimicrobial agents	Zone of inhibition (mm, mean \pm SD)
Fluconazole	18 \pm 0.03
ZnO NPs	9 \pm 0.14
CS	6 \pm 0
ZnO/CS/VA	31 \pm 0

Evaluating and calculating MBC and MFC values are essential when measuring the viability of microorganisms after exposure to compounds. In the current study, both the MIC and MFC values of ZnO/CS/VA were found to be 5 μ g/mL against *C. albicans*, indicating a dose-related inhibitory effect (Figure 7). Fluconazole showed an MIC value of 25 μ g/mL and an MFC value of 30 μ g/mL against *C. albicans*. In contrast, other reports have documented the antifungal activity of ZnO NPs and ZnO/CS nanocomposite against *C. albicans* with MIC values of 200 μ g/mL and 75 μ g/mL, respectively [6, 31].

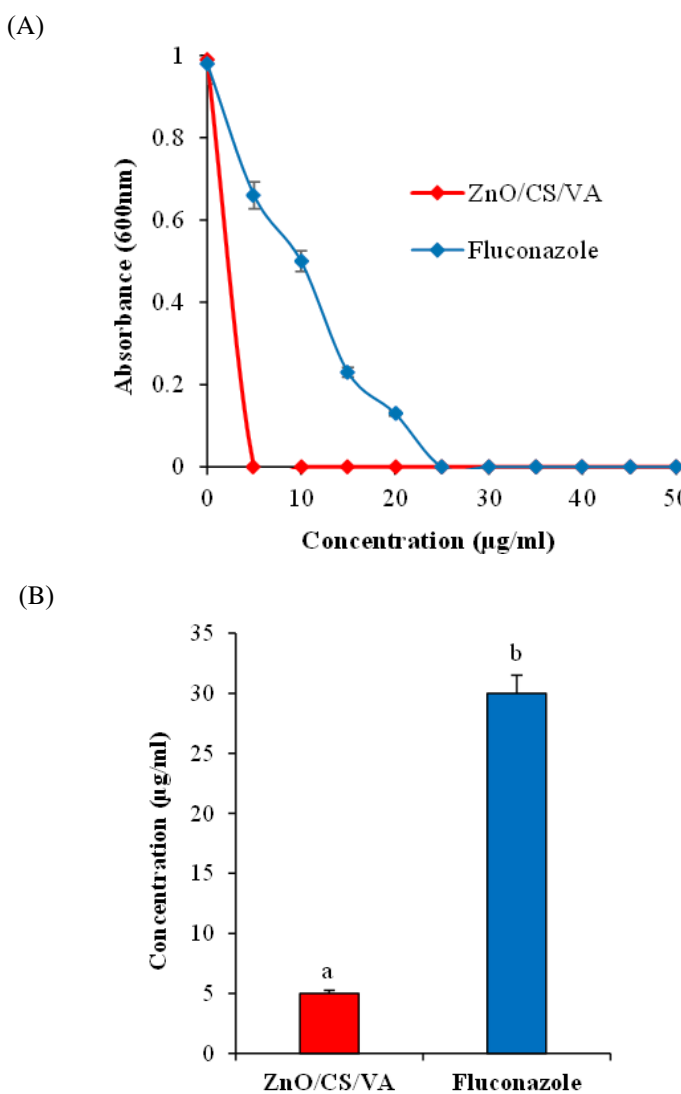


Figure 7 Minimum inhibition concentration; (MIC), (A) minimum fungicidal concentration; (MFC) of ZnO/CS/VA and (B) against *C. albicans* compared to fluconazole.

The anticandidal action of ZnO/CS/VA on the ultrastructure of *C. albicans* was investigated using TEM (Figure 8). Micrograph of untreated *C. albicans* cells (Figure 8(A)) showed a uniformly dense and homogeneous microstructure with intact cytoplasm, small vacuoles, and a normal cell wall and membrane. On the other hand, ZnO/CS/VA-treated *C. albicans* cell micrograph (Figure 8(B)) showed significant changes in the yeast cell contents. These alterations included irregular and malformed forms, leakage of cytoplasmic matrix, separation of cell wall and membrane, a wrinkled appearance of the cell wall, and the formation of large vacuoles in the

ZnO/CS/VA-treated bacterial cells. Although the exact mechanisms of ZnO's antimicrobial action are unknown, scientists have proposed a few potential microbicidal effects. These include the release of zinc ions, which are connected to the accumulation of NPs into microbial cells. The electrostatic interactions between ZnO NPs and cell walls can lead to the destruction of microbial cell integrity and the production of reactive oxygen species (ROS). Smaller NPs may enter microbial cells more readily, resulting in increased ROS production. This can cause cell damage, protein denaturation, and ultimately, cell death.

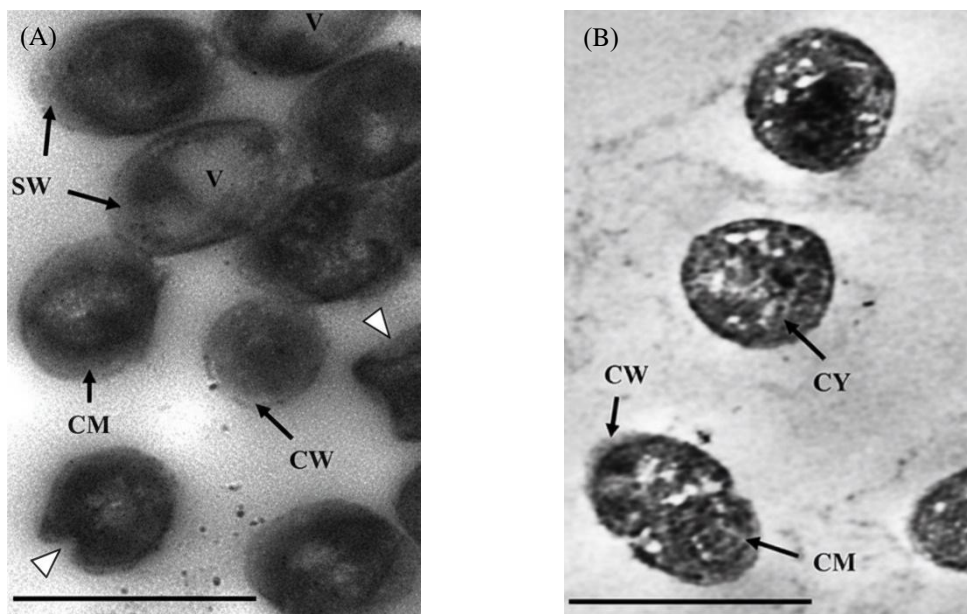


Figure 8 Anticandidal action of ZnO/CS/VA on (A) the ultrastructure of *C. albicans* cells, (B) comparing to untreated cells. CW is cell wall. CM is cytoplasmic membrane. CY is cytoplasm. SW refers to a separation between the cell wall and the cytoplasmic membrane. V is a vacuole. White arrowheads indicated the presence of malformed cells.

4. Conclusions

The current study demonstrates a simple green approach for preparing ZnO/CS/VA using *B. licheniformis* as a stabilizer and reducing agent. The formation of ZnO/CS/VA was confirmed through UV-Vis spectroscopy (348 nm), XRD (31.77°, 47.54°, 56.60°, 66.38°, and 75.48°), FT-IR (stretching vibrations of ZnO at 460-800 cm⁻¹), zeta potential analysis (-17.8 mV), and TEM (spherical-shaped NPs with an average diameter of 78 ± 2.3 nm). The green-synthesized ZnO/CS/VA demonstrated potent anticandidal activity against *C. albicans*, with MIC and MFC values of 5 µg/mL. In comparison, fluconazole had an MIC value of 25 µg/mL and an MFC value of 30 µg/mL. This is the first report to our knowledge, showing that ZnO/CS/VA exhibits strong antimicrobial properties *in vitro*. Therefore, ZnO/CS/VA may be considered a potential candidate for use for future biomedical applications. Future work could involve further investigating the toxicity of ZnO/CS/VA through *in vitro* and *in vivo* studies using an animal model.

5. Ethical approval

The study was carried out in accordance with the guidelines and regulations of the scientific research ethics committee, Faculty of Science, Damietta University, Egypt. This article does not contain any studies with human or animal subjects.

6. Acknowledgements

The authors would like to thank the Botany and Microbiology Department of Damietta University's Faculty of Science for providing the facilities required to conduct this work.

7. Conflicts of interest

The authors report no conflicts of interest in this work.

8. Author contributions

Contribution the idea and the design of the study: ZAB, MIA, and MME. SME and MME conducted the experiments. SME and MME performed statistical analysis and presented data in figures and tables. Supervision: ZAB, MIA, and MME. ZAB, MIA, MME, and SME wrote the draft of the manuscript. All authors read and approved the manuscript.

9. References

- [1] Monaco A, Caruso M, Bellantuono L, Cazzolla Gatti R, Fania A, Lacalamita A. Measuring water pollution effects on antimicrobial resistance through explainable artificial intelligence. *Environ Pollut.* 2025;367:125620.
- [2] Ayukekpong JA, Ntemgwa M, Atabe AN. The threat of antimicrobial resistance in developing countries: Causes and control strategies. *Antimicrob Resist Infect Control.* 2017;6(1):47-49.
- [3] Ranjbar R, Alam M. Global burden of bacterial antimicrobial resistance in 2019: A systematic analysis. *EBN.* 2024;27:16-22.
- [4] Walsh TR, Gales AC, Laxminarayan R, Dodd PC. Antimicrobial resistance: Addressing a global threat to humanity. *PLOS Med.* 2023;20(7):e1004264.
- [5] Kennedy MJ, Volz PA. Ecology of *Candida albicans* gut colonization: Inhibition of *Candida* adhesion, colonization, and dissemination from the gastrointestinal tract by bacterial antagonism. *Infect Immun.* 1985;49(3):654-663.
- [6] Ghosh M, Mandal S, Roy A, Chakrabarty S, Chakrabarti G, Pradhan SK. Enhanced antifungal activity of fluconazole conjugated with Cu-Ag-ZnO nanocomposite. *Mater Sci Eng C.* 2020;106:110160.
- [7] Abou-Dobara MI, Kamel MA, El-Sayed AKA, El-Zahed MM. Antibacterial activity of extracellular biosynthesized iron oxide nanoparticles against locally isolated β -lactamase-producing *Escherichia coli* from Egypt. *Discov Appl Sci.* 2024;6(3):113-115.
- [8] El-Fawal M, A. El-Fallal A, I. Abou-Dobara M, K.A. El-Sayed A, El-Zahed MM. Preparation, characterization, and antibacterial activity of newly biosynthesized ampicillin/chitosan/selenium nanocomposite (AMP/CS/SENC) using *Fusarium fujikuroi* PP794203 against multidrug-resistant *Escherichia coli* PP797596. *J Microbiol Biotechnol Food Sci.* 2024;14(3):e11608.
- [9] El-Harairey MA, Saad HR, Moawed EA, Elafndi RK, Eissa MS, El-Zahed MM, et al. Evaluation of titanium dioxide/catechol polyurethane composite for antimicrobial resistance and wastewater treatment. *Discov Mater.* 2024;4(1):66-69.
- [10] El-Zahed MM, Abou-Dobara MI, El-Khodary MM, Mousa MMA. Antimicrobial activity and nanoremediation of heavy metals using biosynthesized CS/GO/ZnO nanocomposite by *Bacillus subtilis* ATCC 6633 alone or immobilized in a macroporous cryogel. *Microb Cell Fact.* 2024;23(1):278-281.
- [11] El-Fallal AA, Abou-Dobara MI, El-Sayed AKA, El-Fawal MF, El-Zahed MM. Green synthesis, optimization and antifungal activity of Se NPs using *Fusarium fujikuroi* MED14. *Sci J Damietta Fac Sci.* 2024;14(3):57-65.
- [12] Fayed RM, Mohamed Baka ZA, Farouk BH, El-Zahed MM. Antibacterial and cytotoxic activities of a newly green synthesized ZnO/Se nanocomposite combined with *Washingtonia robusta* H. Wendl fruit extract. *Biocatal Agric Biotechnol.* 2025;64:103500.
- [13] Majumder DD, Banerjee R, Ulrichs CH, Mewis I, Goswami A. Nano-materials: Science of bottom-up and top-down. *IETE Technical Review.* 2007;24(1):9-25.
- [14] Mohamed EA, El-Zahed MM. Anticandidal applications of selenium nanoparticles biosynthesized with *Limosilactobacillus fermentum* (OR553490). *Discover Nano.* 2024;19(1):115-120.

[15] Fayed RM, Elnemr AM, El-Zahed MM. Synthesis, characterization, antimicrobial and electrochemical studies of biosynthesized zinc oxide nanoparticles using the probiotic *Bacillus coagulans* (ATCC 7050). *J Microbiol Biotechnol Food Sci.* 2023;13(3):e9962.

[16] Abd El-Nour AT, Abou-Dobara MI, El-Sayed AKA, El-Zahed MM. Extracellular biosynthesis and antimicrobial activity of *Bacillus subtilis* ATCC 6633 zinc oxide nanoparticles. *Sci J Damietta Fac Sci.* 2023;13(2):39–47.

[17] Todorov SD, Ivanova IV, Popov I, Weeks R, Chikindas ML. *Bacillus* spore-forming probiotics: Benefits with concerns. *Crit Rev Microbiol.* 2022;48(4):513–530.

[18] Abinaya M, Vaseeharan B, Divya M, Sharmili A, Govindarajan M, Alharbi NS, et al. Bacterial exopolysaccharide (EPS)-coated ZnO nanoparticles showed high antibiofilm activity and larvicidal toxicity against malaria and Zika virus vectors. *J Trace Elem Med Biol.* 2018;45:93–103.

[19] Gomaa EZ. Microbial mediated synthesis of zinc oxide nanoparticles, characterization and multifaceted applications. *J Inorg Organomet Polym Mater.* 2022;32(11):4114–4132.

[20] El-Fallal AA, Elfayoumy RA, El-Zahed MM. Antibacterial activity of biosynthesized zinc oxide nanoparticles using Kombucha extract. *SN Appl Sci.* 2023;5(12):332-335.

[21] Abd El-Nour AT, Abou-Dobara MI, El-Sayed AKA, El-Zahed MM. Antibacterial activity of optimized extracellular biosynthesized zinc oxide nanoparticles using *Corynebacterium* sp. ATCC 6931. *SJDFS.* 2023;13(3):63–70.

[22] El-Zahed MM, Eissa MS, Moawed EA, El Sadda RR. Application of thiourea polyurethane foam/zinc oxide nanocomposite for anticancer effects and antimicrobial potential. *Discov Appl Sci.* 2024;6(3):112-116.

[23] Fayed RM, Baka ZA, El-Zahed MM. Antibacterial activity of green synthesized zinc oxide nanoparticles using *Washingtonia robusta* H. Wendl fruit extract. *SJDFS.* 2024;14(3):90–101.

[24] Ahmadpour Kermani S, Salari S, Ghasemi Nejad Almani P. Comparison of antifungal and cytotoxicity activities of titanium dioxide and zinc oxide nanoparticles with amphotericin B against different *Candida* species: *In vitro* evaluation. *J Clin Lab Anal.* 2021;35(1):e23577.

[25] Zhang R, Carlsson F, Edman M, Hummelgård M, Jonsson BG, Bylund D, et al. *Escherichia coli* bacteria develop adaptive resistance to antibacterial ZnO nanoparticles. *Adv Biosyst.* 2018;2(5):1800019.

[26] CLSI (Clinical and Laboratory Standards). 27th edition. Performance standards for antimicrobial susceptibility testing. Performance standards for antimicrobial susceptibility testing: Approved standard- twenty-seven Edition. CLSI, Wayne, PA; 2017.

[27] CLSI. (Clinical and Laboratory Standards). 7th edition. Reference method for broth dilution antifungal susceptibility testing of yeasts; approved standard M27-A3. CLSI, Wayne, PA; 2008.

[28] Markus J, Mathiyalagan R, Kim YJ, Abbai R, Singh P, Ahn S, et al. Intracellular synthesis of gold nanoparticles with antioxidant activity by probiotic *Lactobacillus kimchicus* DCY51T isolated from Korean kimchi. *Enzyme Microb Technol.* 2016;95:85–93.

[29] Ali SA, Ali ES, Hamdy G, Badawy MSEM, Ismail AR, El-Sabbagh InasA. Enhancing physical characteristics and antibacterial efficacy of chitosan through investigation of microwave-assisted chemically formulated chitosan-coated ZnO and chitosan/ZnO physical composite. *Sci Rep.* 2024;14(1):9348.

[30] Salman JAS, Kadhim AA, Haider AJ. Biosynthesis, characterization and antibacterial effect of ZnO nanoparticles synthesized by *Lactobacillus* Spp. *J Global Pharma Technol.* 2018;10(03):348–55.

[31] Fozouni L, Tahaei M. Anticandidal effects of zinc oxide nanoparticles on fluconazole-resistant *Candida* isolates causing diarrhea in calves, *in vitro*. *Archives of Razi Institute.* 2023;78(1):499–501.

[32] Sirelkhatim A, Mahmud S, Seenii A, Kaus NHM, Ann LC, Bakhori SKM. Review on zinc oxide nanoparticles: Antibacterial activity and toxicity mechanism. *Nanomicro Lett.* 2015;7(3):219–242.

[33] Mehta M, Allen-Gipson D, Mohapatra S, Kindy M, Limayem A. Study on the therapeutic index and synergistic effect of chitosan-zinc oxide nanomicellar composites for drug-resistant bacterial biofilm inhibition. *Int J Pharm.* 2019;565:472–480.

[34] Iqtedar M, Riaz H, Kaleem A, Abdullah R, Aihetasham A, Naz S. Biosynthesis, optimization and characterization of ZnO nanoparticles using *Bacillus cereus* MN181367 and their antimicrobial activity against multidrug resistant bacteria. *Rev Mex Ing Quim.* 2020;19:253–266.

[35] Aung KK, Htun KT. Preparations and characterizations of chitosan, ZnO nanoparticle and chitosan-ZnO nanocomposite. *J Myanmar Acad Arts Sci.* 2020;18:247-258.